

## Differential NICMOS Spectrophotometry at High S/N

Ronald L. Gilliland<sup>1</sup>

*Space Telescope Science Institute, 3700 San Martin Drive, Baltimore, MD 21218*

**Abstract.** Transiting extrasolar planets present an opportunity for probing atmospheric conditions and constituents by taking advantage of different apparent radii, hence transit depth as a function of wavelength. Strong near-IR bands should support detection of water vapor via G141 spectroscopy of the bright star HD 209458 (H=6.13) by comparing in- and out-of-transit ratios of in- and out-of-band spectral intensity ratios. The reduction and analysis of science observations in which the goal is to support 1 part in 10,000, or better, development of spectral diagnostics using NICMOS grism-based spectroscopy is discussed.

### 1. Introduction

The study of extrasolar planetary atmospheres was initiated five years ago with detection of Sodium in the atmosphere of HD 209458b (Charbonneau et al. 2002) using STIS spectroscopy comparing spectra taken in- versus outside-of-transit. The STIS observations required use of the instrument well beyond its design goals in terms of signal-to-noise and stability, since the signal detected was only at the  $2.32 \pm 0.57 \times 10^{-4}$  level for the relative increase of depth of the Sodium resonance doublet at 589.3 nm during transit.

During a planet transit light is blocked both by the solid body, and possibly by an extended atmosphere. If the extended atmosphere is opaque at some wavelengths, but transparent in others, then relatively more light (hence a deeper transit) will be blocked in the opaque wavelengths. Since atmospheres are generally very thin compared to the planet radius, this type of differential spectroscopy requires the search for small signals. Following proof of concept with the STIS results, it would now be most interesting to detect evidence for primary molecules such as water in extrasolar planet atmospheres. Although some water features exist in the optical, these are in the low QE/high fringing domain for CCDs, but much stronger bands are readily available in the near IR. Water has a strong band near  $1.45 \mu$  (see, e.g., Brown 2001 for predictions of signal strength over wavelengths of 0.3 to  $2.5 \mu$  for transmission spectroscopy of extrasolar planet atmospheres).

As part of qualifying NICMOS and its IR detector for high S/N applications, we had an earlier calibration result in which similar observations were obtained, but only during stable out-of-transit times. The results of this were released in NICMOS ISR 2003-01 (Gilliland and Arribas 2003), and concluded that differential spectrophotometry could be obtained that would support the one part in ten thousand goal. This current report provides an update based upon preliminary analysis of data from GO-9832, PI Tim Brown.

In order to obtain a detection of water vapor we initially considered how this might best be approached with NICMOS. Two primary possibilities for differential study of a feature near  $1.45 \mu$  exist: (1) There is a “Water” filter for NIC 1 with a central wavelength of  $1.45$

---

<sup>1</sup>Based on observations with the NASA/ESA *Hubble Space Telescope*, obtained at the Space Telescope Science Institute, which is operated by the Association of Universities for Research in Astronomy, Inc., under NASA contract NAS 5-26555.

$\mu$  that could be used to observe this band. (2) The NIC 3 G141 grism covering 1.1 to 1.9  $\mu$  could be used to simultaneously span wavelengths both inside and outside the water feature. Once it is realized that the signal sought may be as small as  $10^{-5}$ , requiring detection of  $10^{10}$  photons just to obtain sufficiently small Poisson fluctuations, *and control of all systematic errors to this same small level*, the inadequacy of using a filter becomes clear. To use the 1.45  $\mu$  filter to obtain knowledge of how this feature changes during transit, in comparison to a control band, would require cycling between filters; this in conjunction with the need to take very short exposures to avoid saturation on this  $H = 6.13$  star would not support reaching the desired Poisson limit. Use of the grism provides two essential advantages: (1) The light is dispersed over order 100 pixels, thus allowing a much higher rate of photon collection, and even with instrument defocus HD 209458 reaches half of full well depth in only 2 seconds. (2) By simultaneously observing in- and out-of-band, the ability to correct for systematics, such as instrument sensitive drift, is far superior.

Having decided on the grism, the next decision involved dithering strategy. We explored the possibility of trailing the telescope in the cross-dispersion direction, taking about 60 seconds to trail over 200 pixels would provide the desired exposure to half of full well depth. But, ultimately, this proved impractical, if not impossible, for the ground system to support. The signal that we will pursue here is doubly differential. By this we mean that: (a) we care only about the relative change of brightness between wavelengths in-band (1.35 - 1.55  $\mu$ ) to those in nearby continuum, and (b) we care only about how the latter quantity changes between times during the 3 hour transit to nearby times outside of transit. Since we care only about relative changes, it seems best to dither not at all, if the guiding is expected to be perfectly stable, or to dither only by an amount required to internally calibrate the response to the expected small guiding errors. Were we to dither the spectrum to unique pixels in an attempt to provide more accurate results this would have the effect of mixing in additional errors in the time domain; our best bet is to maintain an essentially constant pointing and take advantage of searching only for differential changes.

## 2. The Observations

With a full width of about 3 hours for the HD 209458b transit, it is possible to obtain equal coverage of times inside and outside transit with four contiguous HST orbits roughly centered on the transit. STIS experience suggested that instrumental stability is much poorer during the first orbit on the new target, our NICMOS experience suggests the same and we adopted the strategy of using five HST orbits to span a planetary transit, but not expecting to utilize the first HST orbit.

Even with dispersion over 100 pixels using the grism, HD 209458 would saturate NIC 3 in less than 1 second. Since there is a significant overhead associated with new MULTI-ACCUMS, and the minimum exposure time in any case is 0.3 seconds, it is advantageous to use moderate defocus. We chose an offset of -0.5 mm for the PAM to provide a FWHM of about 5 – 6 pixels in the cross dispersion direction. This sacrifices spectral resolution at the level of a factor of 2 – 3, but allows “longer” exposure times of 1.99 seconds to be used in which the exposure reaches only half of full well depth. Using STEP1 MULTIACCUMS with NSAMP = 4, this defocus yields spectra with peak per pixel count levels of 70,000 e-, or about 400,000 e- after summing over cross dispersion. Even with using a spectral element to spread the image over many pixels along the dispersion direction, using significant defocus, and adopting a MULTIACCUM option with a small number of samples the duty cycle (fraction of available exposure time during which photons are actually collected) is only 18%. The latter implies, that should this general approach work, then significantly fainter stars could be observed without an initially equal loss of sensitivity, since much larger duty cycles could be used.

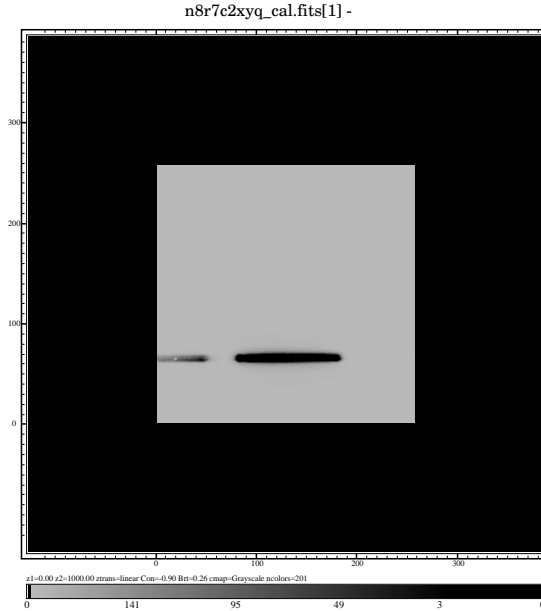


Figure 1: A G141 spectrum from GO-9832. The first order spectrum of interest is in the lower, center part of NIC 3, and was placed on a relatively clean (in terms of pixel quality) portion of the detector.

A typical example (one of 3,142 used) of a pipeline `cal.fits` data product is shown in Figure 1. The data for GO-9832 consists of 3 visits (observed in 2003, 2004, and 2005), each of 5 orbits roughly centered on the 3-hour planetary transit. About 250 exposures are obtained per HST orbit.

### 3. Data Reductions

The grism data are not flat-fielded as part of the pipeline reductions, since the appropriate flat would be wavelength dependent and dependent upon the distribution of sources in the field of view. In our case, with just a single point source, we have used the reference dispersion solution for G141 to provide wavelengths for each column in the first order spectrum. Then the current on-orbit flats for F108N, F113N, F164N, F166N, F187N, F190N and F196N are used to fit the wavelength dependence of the flats as a quadratic function at each pixel. The resulting quadratic was then evaluated at the appropriate wavelength by column and applied as a multiplicative correction for all pixels to be summed over in the spectral extraction. This worked very well with *rms* residuals over the 7 flats usually at the 0.001 level. Outside of the pixel area dominated by the first order spectrum, I simply adopted the F160W flat field to represent a wavelength integrated mean.

Regions well away from the spectrum (and ghosts) were chosen to allow provision of a mean, per-frame background (determined from sigma-clipped averages) which was then subtracted globally. Inspections have been made to determine if pedestal corrections need to be applied, for these ultra-high S/N observations a correction for pedestal does not seem necessary. Pixels within the spectral extraction region that are either dead or noisy have been identified and interpolated over in each individual frame (identified from both the data quality array and close inspection of the data, including ‘chi-squared’ maps of variance over a stack of nominally identical images).

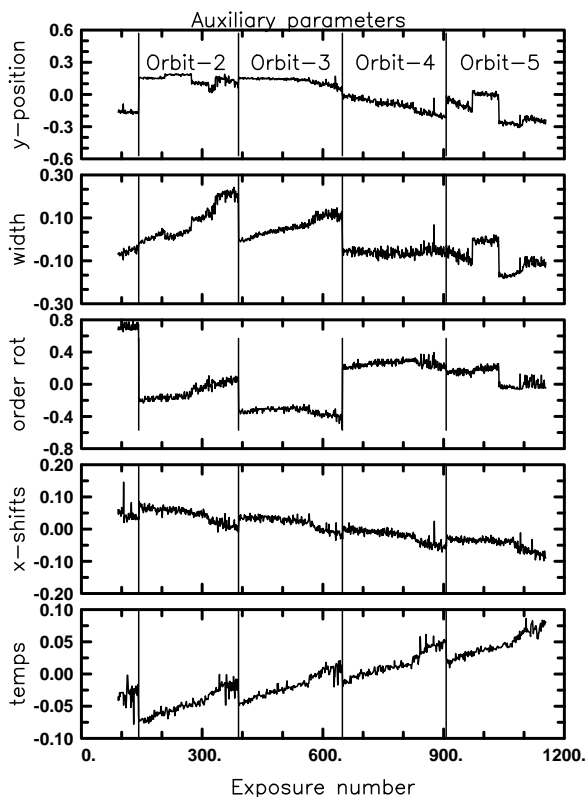


Figure 2: Variations of external parameters for from top: y-position (cross-dispersion placement in pixels), width of the spectrum (Gaussian fit in pixels), spectrum rotation from one end to the other, x-position (from cross-correlation of extracted spectra), and temperature of the detector. Data from the 5 orbits are concatenated together for display purposes, vertical lines indicate the separate orbits.

Intensities are extracted as a simple aperture sum over the first order spectrum (up to a 20 pixel wide extraction box has been used to include most of the stellar flux). Measurements of spectral y-positions, cross-dispersion widths, and order rotation (along x) are obtained by fitting a Gaussian in cross-dispersion at many columns along the spectra, then averaging these. Exposure-to-exposure shifts in dispersion are obtained by cross-correlating individual extracted spectra with a mean spectrum. The temperature record in use was provided by Eddie Bergeron.

Two time series are of interest. The first is simply the direct intensity which shows the transit feature as a 1.6% dip. The second is the ratio of Water-band to nearby continuum band with removal of, and normalization by the mean value. Evidence of extra absorption within the water band would thus appear as a depressed value for this index during transit. Minor changes of spectrum positioning on the detector, etc., may induce changes in the time series, we therefore apply a cleaning step of decorrelating the time series variations of intensity with changes in these external parameters. Figure 2 shows the change of these over time for Visit 02. The process is: 1) evaluate a linear least-squares fit correlating the time series during orbits 2 and 5 (outside of transit) only as a function of the 5 external parameters, then 2) evaluate the model for all times and subtract from the time series in question.

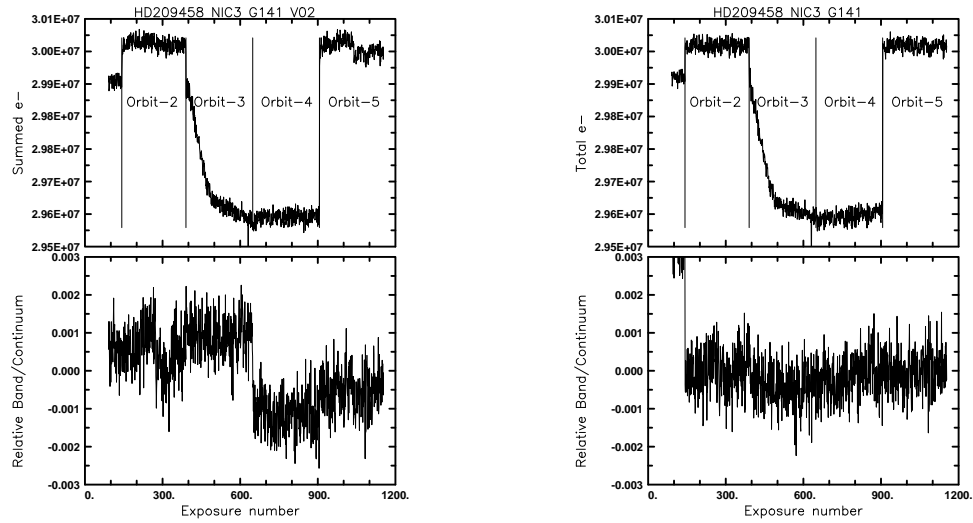


Figure 3: Left panels show the direct (top) and water-band to continuum ratio (bottom) time series after initial creation. The right panels show the same after the decorrelation step with parameters shown in Figure 2.

The before and after decorrelation time series for both the direct sum, and water-band to continuum ratio are shown in Figure 3. Except for the remaining unique behavior of orbit 1 (expected), the decorrelated time series are much cleaner.

#### 4. Nonlinearity Test

During the planetary transit the direct intensity falls by 1.6%. Since the NICMOS detectors are known to have small nonlinearities in response to exposure level, and we wish to push these data to the levels allowed by Poisson statistics (which will be of order  $10^{-5}$  for the ratio of in-water-band to continuum during, versus out-of-transit) an independent check of nonlinearity is advisable. An error of only  $10^{-5}/0.016 = 6 \times 10^{-4}$  in the linearity correction (differential between pixels within water band and neighboring continua) would be of concern here.

During the first orbit of each visit we obtained four series of 10 exposures at each of MCAMRR, NSAMP = 6 and 7 interleaved with the standard STEP1, NSAMP = 4 observations, thus providing relative exposure times of 1.82, 2.11 and 1.99 seconds respectively. Figure 4 shows the results of combining data for all of the available test observations to constrain the linearity. After forming sums in the Water-band normalized to continua as would be done in the standard observations we find a constraint on the nonlinearity induced signal at  $1.5 \times 10^{-5} \pm 1.5 \times 10^{-5}$ . This result is consistent with zero and near the limiting precision available from the primary data to measure the evidence for water in the HD 209458b atmosphere. The linearity correction for count level applied in the pipeline is quite good for our purposes.

An item requiring future investigation is whether the recently detected nonlinearity with count *rate* (“Bohlin” effect) could be a limiting systematic to contend with.

#### 5. Time Series Photometry – Comparison with STIS

Figure 5 shows overplotted results for both STIS (from Brown et al. 2001) and NICMOS time series. The STIS spectra centered at 600 nm provided a time-series *rms* of  $1.1 \times 10^{-4}$

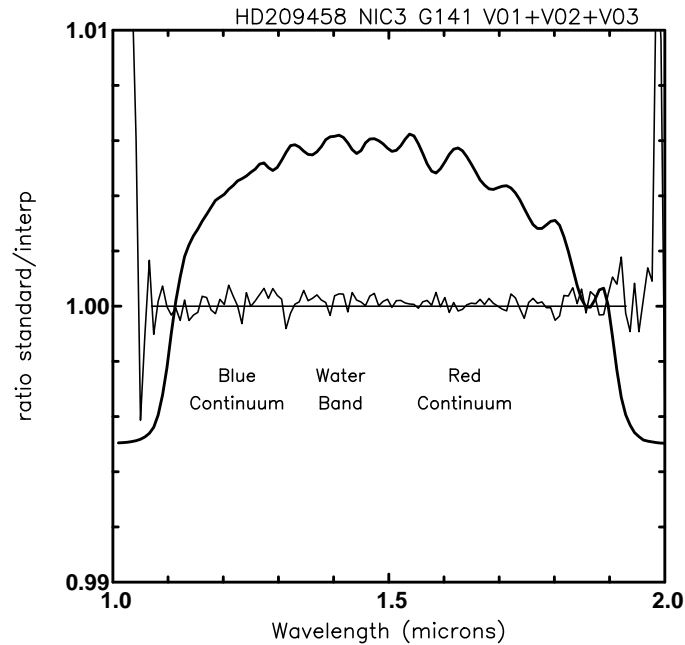


Figure 4: Mean of spectra ratios (multiplied by inverse ratio of exposure times at  $t_{exp} = 1.82$  to  $1.99$ s and  $1.99$  to  $2.11$  s plotted as the thin curve. The overplotted heavy curve offset from unity simply illustrates the relative count levels over the grism spectra. There seems to be little if any residual nonlinearity over the spectral domain of interest.

at an 80 s cadence (30% above the Poisson limit for count level of  $1.55 \times 10^8$  electrons). Rebinned to 80 seconds the NICMOS photometry provides an  $rms$  of  $1.8 \times 10^{-4}$ , about  $\times 2.4$  above the Poisson noise limit ( $2.16 \times 10^8$  electrons detected each 80 s). The noise level on the purely differential index tracking water to continuum bands is closer to being Poisson limited.

## 6. Summary

With the current loss of STIS on *HST*, the NICMOS grisms provide the best spectroscopic capability for probing atmospheres of extrasolar planets. The presence of broad absorption features, particularly from water vapor, relative to any similar diagnostics in the optical would make NICMOS competitive for current advances, even if STIS had not been lost. The latter of course requires that, like STIS, NICMOS be able to provide data well outside of its design goals in terms of signal-to-noise and stability.

The analyses discussed here have not yet reached as near fundamental precision limits, as was the case for STIS. At a time series signal-to-noise of 5,500 per 80 second sum ( $< 0.0002$   $rms$ ) for direct photometry summed over the full bandpass, the results are probably far better than could be obtained from the ground, and will be useful for constraining basic system parameters through detailed modeling of the transit light curve. Application of more sophisticated analysis techniques (e.g. difference image analysis) may allow superior results to still be obtained. For the index of water vapor band to continuum counts the current results are already closer to fundamental limits on this very bright star, and should provide interesting constraints on the HD 209458b atmospheric water vapor content.

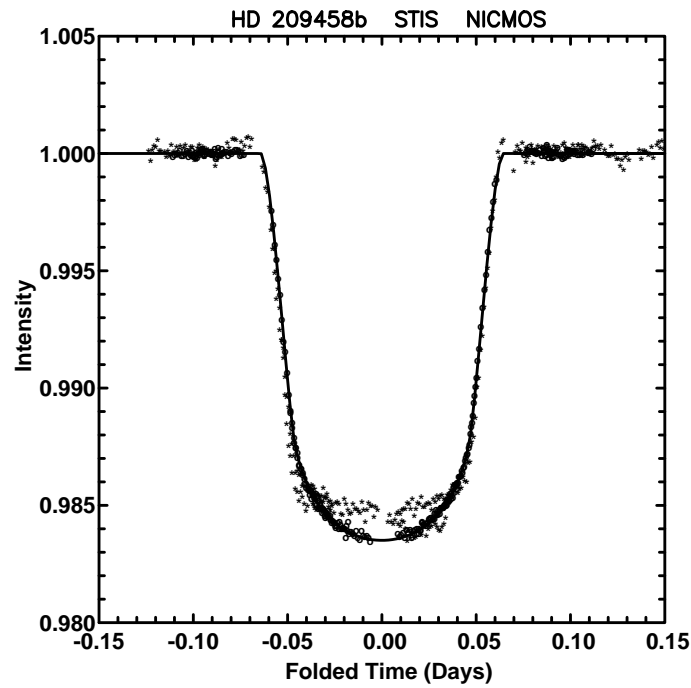


Figure 5: Shows relative intensity through multiple transits from the STIS observations in 2000 ‘o’, and the NICMOS observations in 2003 ‘\*’. The much more rounded bottom to the transit in the STIS (optical) observations is expected from larger limb darkening in the optical than in the IR which should (as generally observed) yield a flatter eclipse bottom.

**Acknowledgments.** I thank Santiago Arribas, Eddie Bergeron, and Tim Brown for discussion and input on a wide range of topics.

## References

- Brown, T.M. et al. 2001, *ApJ*, 552, 699
- Brown, T.M. 2001, *ApJ*, 553, 1006
- Charbonneau, D. et al. 2002, *ApJ*, 568, 377
- Gilliland, R.L., and Arribas, S. 2003, *Instrument Science Report NICMOS 2003-0* (Baltimore:STScI), available through <http://www.stsci.edu/hst/nicmos>